Mesoporous Alumina Mediated Synthesis of Perovskite Nanocrystals and their Photophysical studies

Daimiota Takhellambam

MS13101

A dissertation submitted for the partial fulfilment of
BS-MS dual degree in Science

Indian Institute of Science Education and Research Mohali

April 2018

Mesoporous Alumina Mediated Synthesis of Perovskite Nanocrystals and their Photophysical studies

Daimiota Takhellambam

MS13101

A dissertation submitted for the partial fulfilment of
BS-MS dual degree in Science

Indian Institute of Science Education and Research Mohali

April 2018

Certificate of Examination

This is to certify that the dissertation titled "**Mesoporous Alumina Mediated Synthesis of Perovskite Nanocrystals and their Photophysical studies**" submitted by **Mr. Daimiota Takhellambam** (Reg. No. MS13101) for the partial fulfilment of BS-MS dual degree programme of the institute, has been examined by the thesis committee duly appointed by the institute. The committee finds the work done by the candidate satisfactory and recommends that the report be accepted.

Dr. Ujjal K. Gautam   Dr. Sanchita Sengupta   Dr. Debrina Jana

(Supervisor)

Dated: 20th April 2018

Declaration

The work presented in this dissertation has been carried out by me under the guidance of Dr. Debrina Jana at the Indian Institute of Science Education and Research Mohali. This work has not been submitted in part or in full for a degree, a diploma, or a fellowship to any other university or institute. Whenever contributions of others are involved, every effort is made to indicate this clearly, with due acknowledgement of collaborative research and discussions. This thesis is a bonafide record of original work done by me and all sources listed within have been detailed in the bibliography.

Daimiota Takhellambam

(Candidate)

Dated: April 20, 2018

In my capacity as the supervisor of the candidate's project work, I certify that the above statements by the candidate are true to the best of my knowledge.

Dr. Debrina Jana

(Supervisor)

Acknowledgement

List of figures

List of tables

Abbreviations and Acronyms

1. PNCs -   Perovskite nanocrystals

2. PL –   Photo Luminescence

3. PL-QY -   Photo Luminescence-Quantum YielD

4. RT -   Room temperature

5. TCSPC -   Time Correlated Single Photon Count

6. DMF -   N,N-Dimethyl Formamide

7. MA -   Methylammonium cation

8. FA -   Formamidinium

Contents

ABSTRACT

Metal halide perovskites are new class of compounds which has intrinsic defect tolerant property and belong to a group of bright emitters. Lead halide Perovskite with the formula AMX_3 having similar structure are reported to possess high photoluminescence quantum yield which can cover up a large color gamut. They are classified as effective absorbers of light which can be subjected in applications of photovoltaics. However, working on nano scale of these perovskite nanocrystals has been a challenge due to several factors including stability, moisture dependency, high temperature requirement and agglomeration tendency of the nanocrystals. Our main emphasis is to produce perovskite nano crystals of both pristine $CsPbBr_3$ and Br-I mixed nano crystals in a thin film form using alumina as the mesoporous template keeping in view real world applications. Another crux of our work focuses on the exchange of anion (halide counterpart) of the solid PNC to get PNCs of different compositions having band gap tenability over the visible spectral range. This work also reports the improved stability of iodine rich PNCs of more than 120 minutes at room temperature in air. This can be attributed to the confinement of PNCs inside mesoporous network.

CHAPTER 1

INTRODUCTION

1.1 Perovskites and defect tolerance

A class of compounds with the crystal structure formula AMX_3 is under the name Perovskite. A is the organic/Inorganic cation (MA^+-methyl ammonium, FA^+-formamidinium), M is the metal cation (Pb^{2+}, Sn^{2+}, Ge^{2+}) and X is the halide anion (Cl^-, Br^-, I^-)[1] Protesque et al[1] for the first time reported novel synthesis of Cesium lead halide inorganic perovskite nano particles with a PL-QY of 90%. Figure1 shows the pictorial representation of the arrangement of the atoms in a cubic crystal.
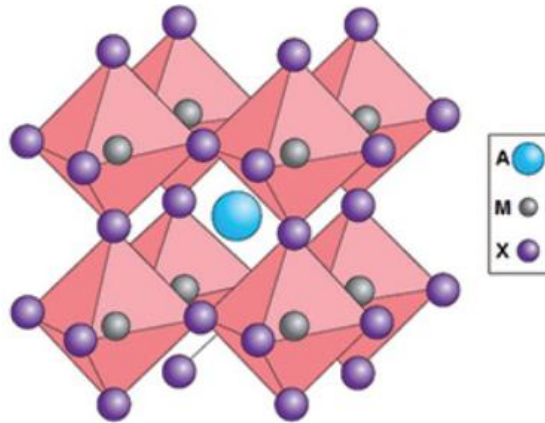
Fig 1: AMX_3 cubic crystal arrangement of cations and anions (Taken from Ref 2)

Metal halide perovskite has been in the spotlight of bright emitters which spans the entire visible region of the electromagnetic spectrum. Colloidal cesium lead halide QDs has been on research bench owing to its optoelectronic properties and defect tolerant nature. The dangling bonds on the surface of the nano crystal which are non-bonding in nature give rise to defect states which can trap charge carriers inhibiting the optoelectronic processes. In Perovskites, the situation differs by a rare situation where the intrinsic defects do not act as defect charge trapping site which is due to the electronic band structure. Metal ions with 2 electrons in s orbital leads to the formation of valence band maximum and conduction band minimum fig 2 with antibonding states, in addition the strong spin-orbit coupling stabilizes the formed conduction band minimum.[3-17]
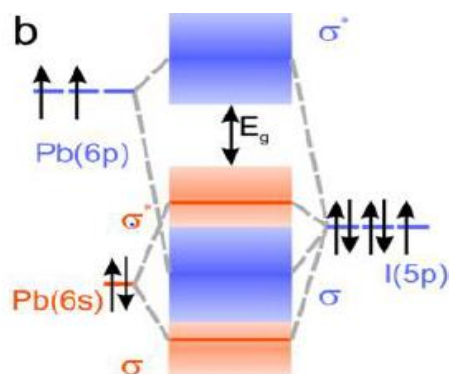
Figure 2. Hypothetical defect-tolerant band structure [pic ref 20]

These two aspects reduces the formation of defect states in perovskite nano crystals and proves to be a better option than the conventional Quantum Dots The tunable optical properties of the perovskite nano crystals are attributed to their permissible compositional modifications, size and shape. Substitutions of the cationic A part with FA and the metal cation part with Sn leads to the changes has been investigated.[18]

1.2 Approaches made till date

1.2. a Solution phase synthesis

Solution based colloidal synthesis of mono-dispersed 4-15 nm $CsPbX_3$ pure halide and mixed halide composites with cubic shape and cubic phase perovskite crystal structure has been reported with high PL-QY of 50-90%. [19]
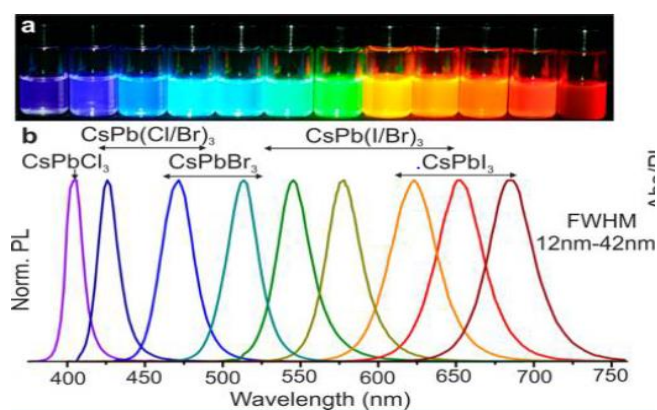
Fig3: Colloidal perovskite CsPbX3 NCs (X = Cl, Br, I) size- and composition-tunable band gap energies covering the   entire visible spectral region λ = 365 nm (Taken from Ref 19)

The reported synthesis is by hot injection method where the two precursors of the perovskite are reacted at high temperature inside an inert atmosphere in

presence of ligands. The mixing of the halide compositions makes it possible to tune the emission peaks in the entire visible spectra.

1.2. b Mesoporous powder template based synthesis

Template assisted growth of PNCs research has been investigated by Maksym V. Kovalenko et al [20] where the synthesis of PNCs was operated using mesoporous powder silica matrixes as templates, showing the ligand-free non colloidal way of preparation and tune the band energy of the nanocrystals with respect to the size of the mesopores employed.

Fig4: Schematic of the template-assisted synthesis of APbX3 NC in mesoporous silica and images of perovskite solution impregnated mesoporous silica in daylight and under UV illumination (Taken from Ref 20)

To completely dry the solvents a temperature of above 150^0 C in inert atmosphere is employed. The major finding in their work is the outstanding PL with tunable emission peak from green to near infrared region with high PL-QY of above 50%. Fig 4 shows the photograph of mesoporous powders incorporated with perovskites under UV illumination and under day light.

1.2. c Vapor phase synthesis

Vapor phase synthesis of perovskite nano crystal has been studied to precisely tune the thickness of the film and make its applicability to solar cell device. The co-sublimation of the precursors by alternating the layers between the two layers in an inert environment in the synthesis makes it an easy way to control the thickness of the film developed. $CsPbI_3$ has been successfully frozen in inert atmosphere by rapid cooling way

from yellow, orthorhombic to black color, cubic phase transition at 300^0 C by cooling on a metal surface upon seeing the transition.[21]
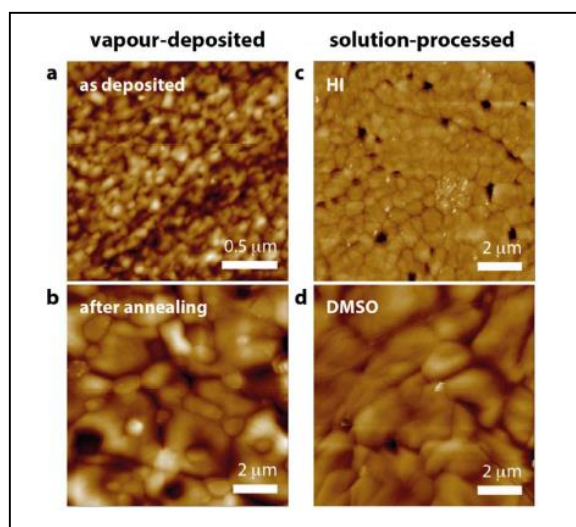
Figure 5: AFM images of (a-b) vapor-deposited $CsPbI_3$ before (a) and after (b) annealing and (c-d) spin-coated CsPbI3, using HI (c) or DMSO (d) (Taken from Ref 21)

1.3 Mesoporous matrix

Porous materials in the size range of 2 to 50 nm are termed as mesoporous materials. Pores greater than 2 nm are microporous and above 50nm are macroporous. Porous systems has been in the limelight for many purposes including as a template in catalysis, shape control synthesis, drug delivery, separation. Its high surface area and nano scale structural makes it viable for efficient properties. Usage of shape directing agents for the synthesis of mesoporous network [22] has led to the formation of both ordered and disordered network of pores. Alumina has been chosen over other templates because of its high adsorbing nature, tunable thickness from 1 to 3 µm, unreactive to various solvents, crack free property while sintering at high temperature and the cubic crystallinity phase of γ-Al_2O_3 which gets converted at temperature range of 450^0C to 550^0C which is in-phase with the cubic structure forming perovskite nanocrystals.
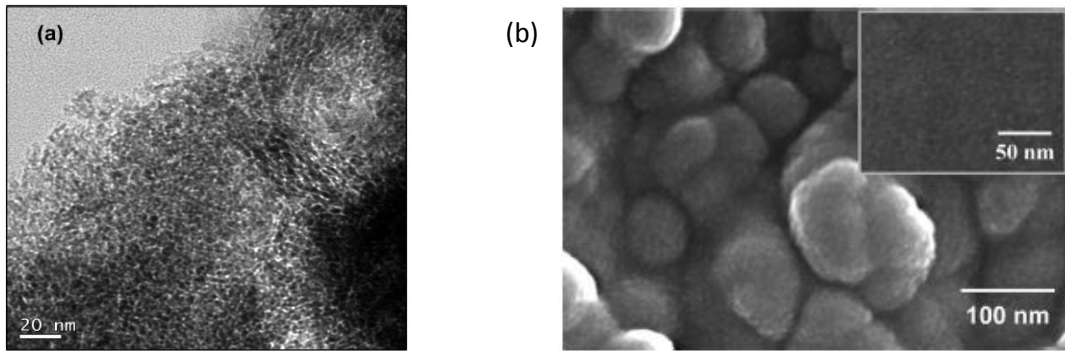
Fig 6: (a) Structure of mesoporous γ-Al₂O₃ film heat-treated at 500 °C (b) FESEM image of surface of the mesoporous γ-Al₂O₃ film heat-treated at 500 °C. (Inset) is the top surface of the film (Taken from Ref 22)

1.4 Applications of Perovskites

Mitzi and co-workers[23-26] has worked on Organic –inorganic perovskite LEDs for the first time, mostly as an active layer. Owing to their interesting tunable optical property by changing their composition, perovskites are used as light absorbers and has been subjected as sensitizers in titania or Zinc oxide based solar cells. The highest efficiency in PCE in perovskite based solar cell is 22.1% to date.[27] The high adsorption coefficient and the intensive work to develop in film deposition has made them a very good candidate for economically viable photovoltaic application serving ingredient till date.[28] Thin film PNCs can also be used in the backlit display of electronic devices.

1.5 Objectives of my work

Research work on perovskite nano crystals has been successfully done in colloidal solution form of synthesis which includes injection of the two precursors in an inert atmosphere at high temperature. Another work in mesoporous powder assisted way of synthesizing various shaped nano crystals to tune the emission spectra over the entire visible spectrum has been successfully reported. Alternative way of PNC synthesis is vapor assisted way of making film form for photovoltaic purposes. PNCs in thin film form can serve as an ingredient for solar cell based devices, LEDs and as the backlit display of electronic devices. Solution based synthesis will face the problem of applying the PNCs solution onto a template which may hinder the uniformity. Vapor assisted way of making films cannot control the size factor of the PNCs. Therefore, a template assisted way of synthesis of PNCs in a thin film form can be an exciting way. Our goal is to develop

5

uniform mesoporous alumina film template and make the PNCs inside the mesopores and study their photophysical properties. Above all, the sintering temperature goes well with the usage of normal borosilicate glass slides which defines the economic point of experimental requirements. The stability of the PNCs is more in the template assisted method due to confinement of the nanocrystals inside the mesopore and uniform distribution over the film surface. Solution based synthesis requires assistance of ligands inside the solution to stabilize the nano crystals whereas mesopore confined nanocrystals are expected to be more stable without any usage of capping agents. Another advantage of the mesoporous template assisted way of synthesis is the prevention of agglomeration of the nanocrystals.
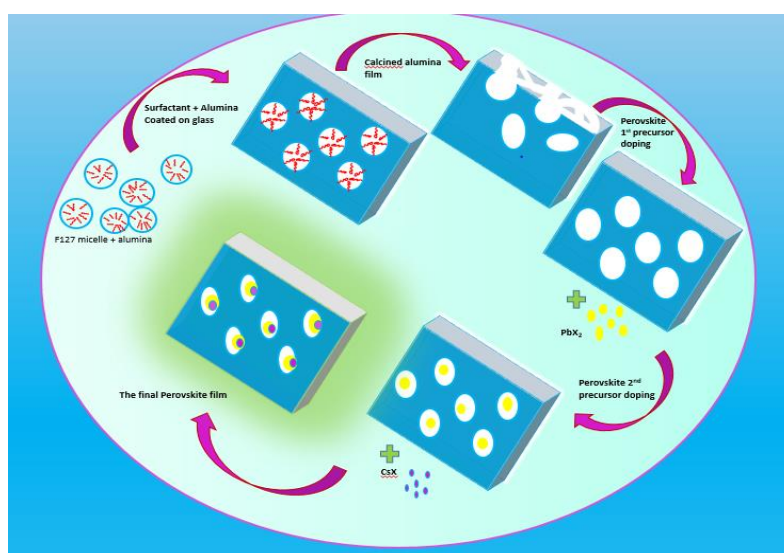

Fig7: Schematic of overall process of PNC incorporation in mesoporous templates

CHPATER 2

Experimental

2.1 Chemicals

ASB (Aluminium Trisecondary Butoxide), Tetrabutyl ammonium iodide (TBAI), cesium hydro oxide(SIGMA), Lead bromide ($PbBr_2$), Lead iodide(PbI_2), Oleic aicd, Oleyl amine, cesium carbonate were purchased from Sigma Aldrich. Hydrochloric acid (HCl, 37% in water) MERCK, methanol (SRL), absolute ethanol 99.9% (RANKEM), 1-propanol(SRL), N,N – dimethylformamide (RANKEM), Isopropyl alcohol (RANKEM), microscope glass slides (Rivera), cesium iodide(RANKEM), hydrobromic acid (48% in H_2O) SRL. The chemicals purchased were used without further purification.

2.2 Precursor synthesis:

Cesium bromide was prepared using the reported protocol.[29] In a typical synthesis, 3.12g cesium carbonate was dissolved in 4.99ml of water in a heating condition of 40^0 C, hydrobromic acid was added until the solution becomes a pH of 3 and boiled at 85^0 C for 1.5 hour. The solution was brought back to a pH of 7 using aqueous cesium hydroxide in water and stirred for 10 more minutes. The solution was filtered using a filter paper and the filtrate was subjected to an evaporation inside oven at 200^0 C. Formed white salt was re-dissolved in water and recrystallized in ethanol and dried in vacuum oven at 60^0 C overnight.

2.3 Boehmite preparation:

10g ASB (1 mol) was poured in 73g of hot water(100 mol) and stirred vigorously at 80^0 C under refluxing condition for 5 hours. After completion of 1hour, a peptization process is performed by adding 0.40g of HCl and made to stir vigorously for further five more hours. On completion of 5 hours, the solution is made to reflux for 30 hours without stirring at a temperature of greater than 80^0 C. Finally we get a transparent solution which is ready for making the coating sol[30]

2.4 Coating Sol preparation:

The gel forming sol was prepared using the synthesized boehmite AlO(OH). First, the obtained solution was concentrated to 7.5 equivalent weight % of $AlO_{1.5}$ using a

rotatory evaporator to distill off 2^0 butanol along with some water. Methanol was added up to dilute the $AlO_{1.5}$ to 5.3 weight%. Surfactant F127 (PEOPPPOPEO) was weighed 0.001 mol% equivalent to the amount of $AlO_{1.5}$ present in the sol and dissolved in 1-propanol. The 5.3 weight % sol was then finally added to the solution of the surfactant to make a final $AlO_{1.5}$ 4 weight % solution, stirred for 1 hour and then aged for 1 day at RT.[30]

2.5 Coating sol preparation process

Glass slides used for coating the alumina sol (25.4mm x 76.2mm x 1.2mm) was first cleaned using detergent water, further it is washed with deionized water and then in ethanol and then boiled in 2- Propanol for 5 minutes.[31] The aged coating sol is stirred to make a solution form and using a dip coater, the cleaned glass slides were coated at a pulling out rate of 140 mm/min. The as coated slides were dried in oven for 15 min at 60^0 C and then subjected for calcination at a control heating rate of 1^0 C till 500^0 C and made to calcine at this temperature for 1 hour and cooled down at natural way without any control.

2.6 Doping solution preparation:

The doping, solutions for the synthesis of the mixed perovskite nanocrystals were prepared in different solvents. For the mixed perovskite, CsBr was paired with counterpart PbI_2 and for CsI with $PbBr_2$. The alumina coated glass slide was doped in the first precursor 0.05 M concentration of lead halide (PbX_2) dissolved in N.N dimethylformamide (DMF) followed by washing with DMF and dried in oven at 60^0 C for 15 min. After cooling down to room temperature, the first precursor doped alumina slide was doped into the second precursor which is a solution of Cesium halide salt CsX (0.05 M) prepared in ethanol and water mixture in 7:1.5 (v/v ratio) and subsequently washed with ethanol. Cesium lead bromide, $CsPbBr_3$ film was prepared by making 0.025 M concentration of $PbBr_2$ in DMF as the first precursor and 0.1 M CsBr in ethanol water mixture. The perovskite nano crystal synthesis was performed in a concentration ratio as given in Table 1. The as prepared films of $CsPbBr_3$ and ($CsI + PbBr_2$) were subjected to dry at room temperature in open air and (CsBr and PbI_2) were kept inside a desiccator for 1 day after washing before characterization. However, the prepared films of ($CsI + PbBr_2$) were heat treated for 6 hours at 100^0 C and immediately cooled down to room temperature by taking it out of the oven.

TABLE 1

Dissolved in DMF	Dissolved in Ethanol: Water Mix (1.5/7)(v/v)	
$PbBr_2$ 0.025 M	CsBr	0.1 M
PbI_2 0.05 M	CsBr	0.05 M
$PbBr_2$ 0.05 M	CsI	0.05M
PbI_2 0.025 M	CsI	0.1M

2.7 Sample preparation for Brunauer–Emmett–Teller (BET) adsorption study:

Alumina coated slides were scratched with the help of blades manually. Doped samples of alumina films with $CsPbBr_3$ were also scratched to make a comparison of the pore volume occupancy by BET analysis of surface area and BJH pore size distribution calculation.

2.8 Solid state anion exchange:

The as prepared films of $CsPbBr_3$ has been subjected to carry out anion exchange reaction in its solid form with the help of capping agents and a concentrated anion source(20 fold halide excess). It is experimented in two ways. Anion source TBAI was prepared 0.5 M in ethanol and the capping agent solution was made by dissolving 1ml of oleic acid and 20 µl of oleylamine in 5 ml of ethanol. Route 1 is dipping the slide into a mixture of anion source TBAI (3ml) with capping agents (2 ml) for 40s. Route 2 is dipping the PNC incorporated slide in capping agent solution for 1 minute and then to the anion source for 40s. All these reactions were performed at RT.

<div align="center">**Characterization**</div>

2.9 Structural analysis

Powder X-ray diffraction was performed on thin films using Rigaku Ultima IV company fully automatic high resolution X-ray diffractometer system equipped with a 3 kW sealed tube Cu K α X- ray radiation (generator power settings 40kV and 40 mA) and Dtex Ultra detector using parallel beam geometry. Figure 9b and 9c were placed in a quartz plate and a scan rate of 2θ from 10^0 to 50^0 with a scan rate of 2^0/min and Fig 9a was taken from 10 to 50^0 at 5^0/min. The nitrogen adsorption-desorption isotherms were obtained with BET Quantachrome instrument at 77K , and BJH(Barrett- Joyner- Halenda) method was used to calculate the pore size distribution of the doped and un-doped samples of alumina films of $CsPbBr_3$.

2.10 Optical analysis:

UV- Vis absorption spectra of the films were measured using UV 3000+ LABINDIA spectrophotometer at the scan rate of 1nm/s (medium speed scan) and wavelength window of 400 - 700 nm. Photoluminescence (PL) spectra was recorded using Horiba Fluromax-4 with slit widths of 1nm x 1.5nm and a scan integration time of 0.5s at an excitation wavelength λ_{ex} = 365 nm for Br rich samples and 420 nm for the Iodine rich samples. The PL lifetime measurements were carried using Horiba DeltaFlex TCSPC at an excitation wavelength using a pico second diode laser of λ_{ex} 375 nm wavelength at a repetition rate of 1 Mhz. The instrument response function (IRF) was recorded using 1% ludox (colloidal silica) solution. For PL-QY, doped glass film in Rhodamine B (standard QY of 68%) of 10^{-5} M was used as reference.

CHAPTER 3

Results and Discussion

3.1 Brunauer–Emmett–Teller (BET) pore surface area analysis

This study was performed to evaluate the surface area and pore-size distribution of the undoped (without PNC, only the mesoporous alumina matrix) and doped (mesoporous alumina matrix with PNC) samples. This will give us an idea about the occupancy of pores by PNC after their generation inside mesopores.
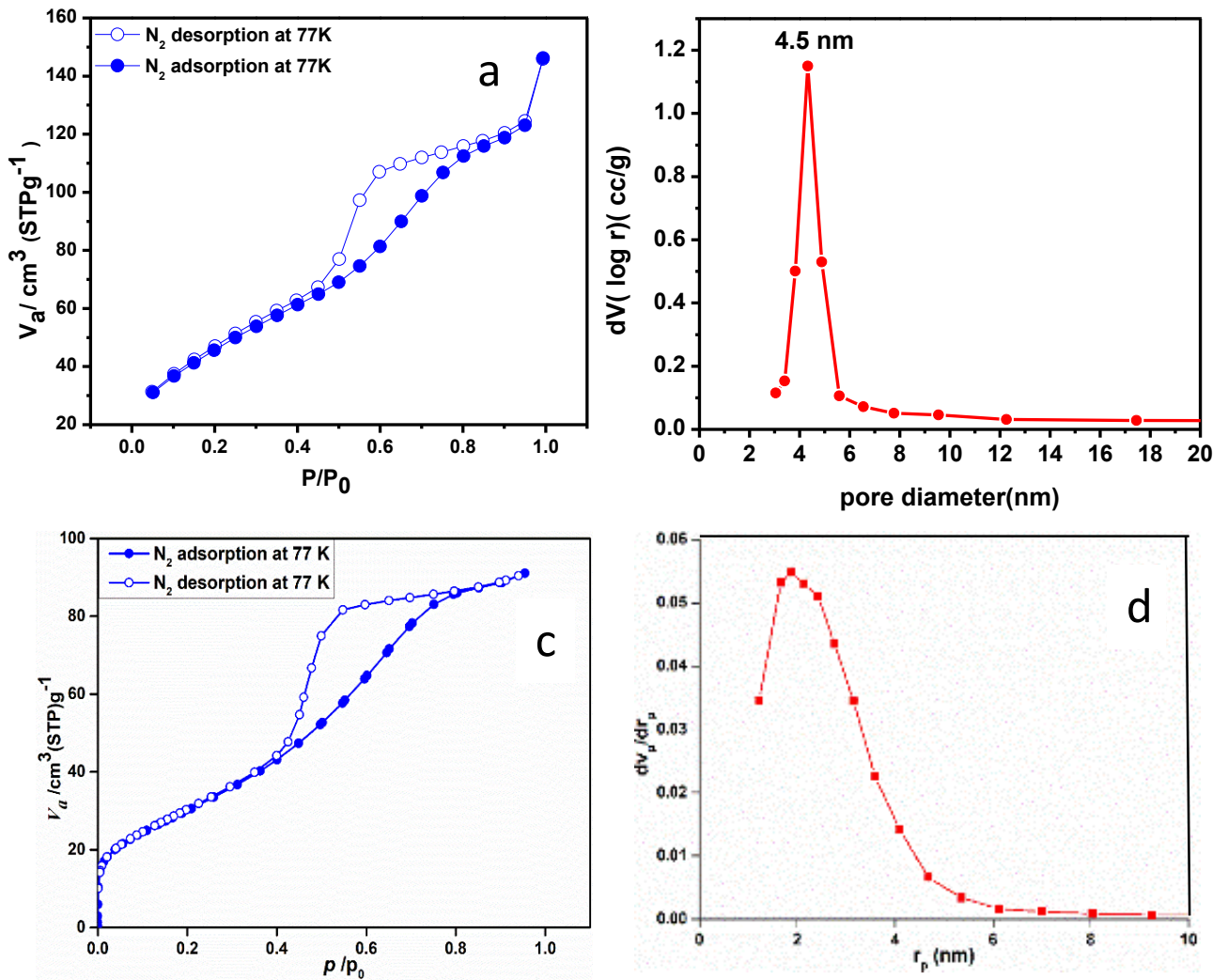

Fig 8: (a) and (c) N_2 adsorption/desorption isotherm of undoped and doped respectively, (b) and (d) pore size distribution of undoped and doped mesoporous alumina samples respectively.

N$_2$ adsorption/ desorption type IV isotherm data for both samples confirm the formation of mesopores with average pore size of 4.5 nm (for undoped) and 4.1 nm (for doped). Table 2 shows the surface area and pore volume of both undoped and doped samples. From the reduction in pore volume data, it can be clearly seen 29.5% of the pores has been occupied by the PNCs.

TABLE 2

Sample	Surface area	Pore volume
Undoped (only alumina matrix)	138.801 m^{2}g^{-1}	0.200 cm^3
Doped (CsPbBr$_3$ NCs incorporated alumina matrix)	117.4 m^{2}g^{-1}	0.141 cm^3

3.2 Powder X-ray diffraction analysis (PXRD)

PXRD data shows the formation of cubic PNCs of CsPbBr$_3$where the peaks are centered around 2θ = 15.8^0 for (100), 21.6^0 for (110), 30.9^0 for (200) planes. These peaks are very close to PNCs <100> <110> <200> spacing in the cubic bulk and with the addition of Iodine to form mixed halide components by introducing Iodine, there is a gradual shift in the peak position which is represented in the Table 3.

TABLE 3

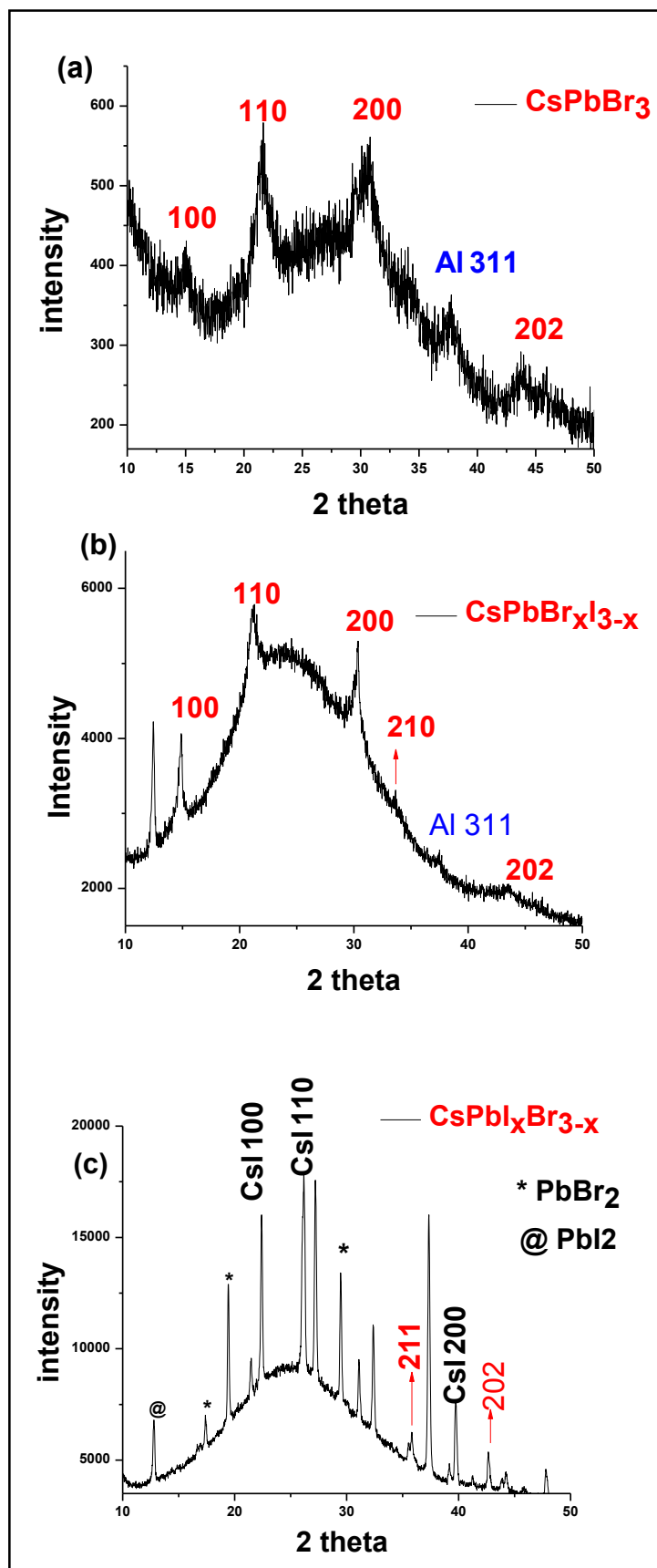| Peak shift	<100>	<110>	<200>	<202>
CsPbBr3	15.08	21.63	30.89	44.08
CsPbBr$_x$ I$_{3-x}$	14.87	21.19	30.35	43.43
CsPbI$_x$ Br$_{3-x}$	---------------	-----------	29.37	42.67

Fig 9: PXRD data of (a) $CsPbBr_3$ (b) $CsPbBr_xI_{3-x}$ (c) $CsPbI_xBr_{3-x}$ with their corresponding (hkl) values.

The cubic phase is confirmed through PXRD but for the third PNC, $CsPbI_xBr_{3-x}$ a mixed phase formation can be the reason for showing intense sharp peaks along with the broad peaks of the PNC. $CsPbI_3$ by itself being very sensitive to moisture and temperature, proper characterization has not been carried out. However similar to the black color phase which is reported to be the perovskite cubic phase of $CsPbI_3$[32] has been successfully frozen in an inert atmosphere shown in fig10. The huge broad peaks is due to amorphous silica which was used as a template for the film preparation.
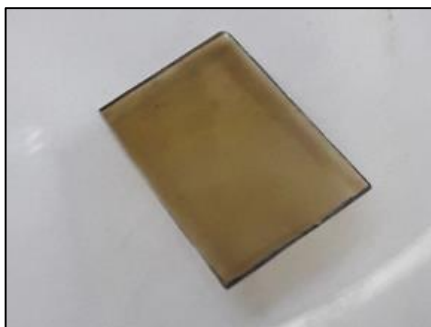

Fig 10: The frozen black colored phase of $CsPbI_3$
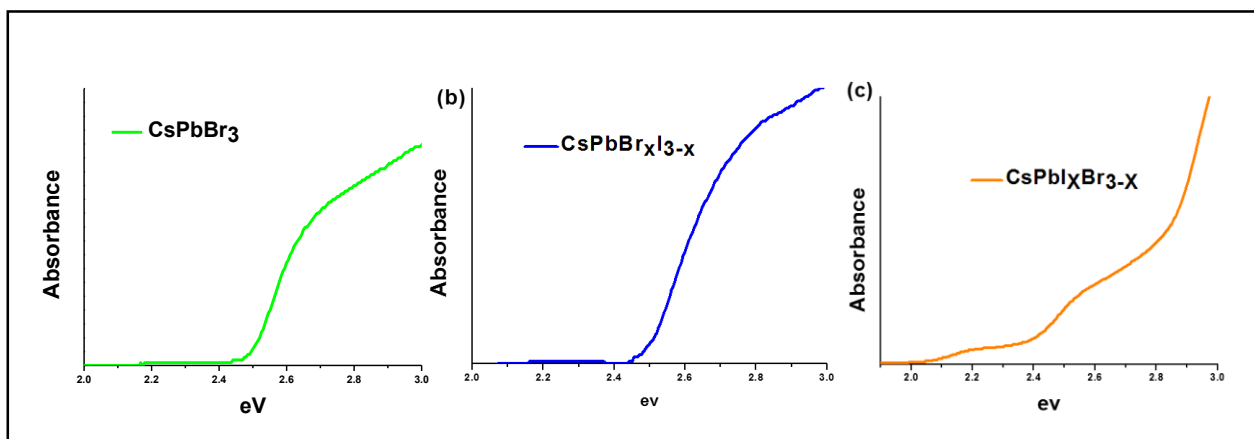
3.3 UV- VIS absorption spectra study

Fig10: UV-VIS spectra of (a) $CsPbBr_3$ (b) $CsPbBr_xI_{3-x}$ (c) $CsPbI_xBr_{3-x}$

Fig 10: show the UV visible absorption spectra of the synthesized PNCs. The data provides the direct optical band gap of the PNCs and using TAUC's plot the band gap energies of the respective NCs in fig (11) have been procured. The UV-VIS graph of fig 10 c hints the formation of other phases on the film.
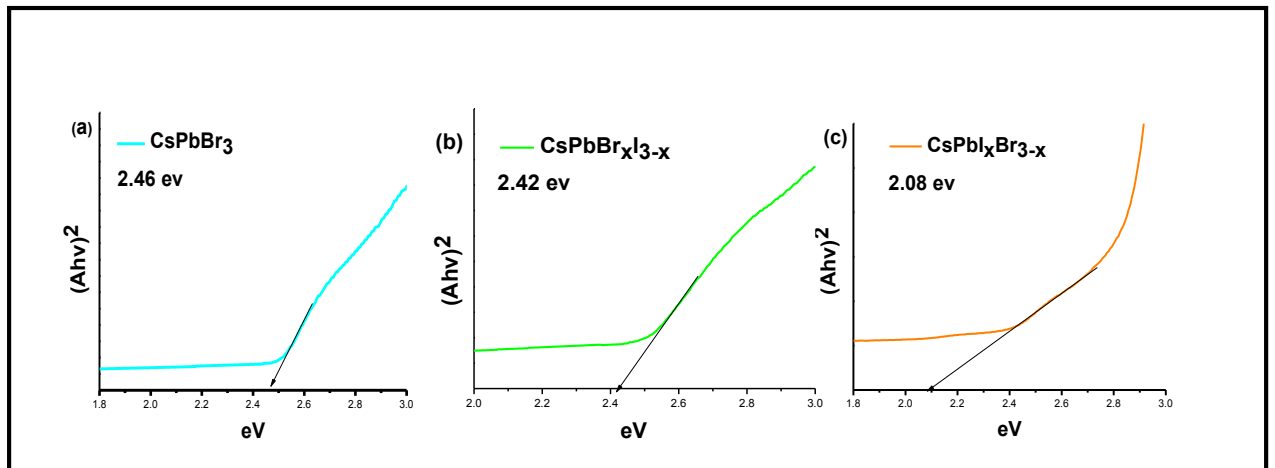
Fig 11: Tauc's extrapolation graphs for band gap determination (a) $CsPbBr_3$

(b) $CsPbBr_xI_{3-x}$ (c) $CsPbI_xBr_{3-x}$

Variations in the band gap energies can be attributed to the surface structure and the local crystallinity of the substrate. With three different compositions, the band gap has been tuned from 2.48 to 2.08 eV. As for the solid state anion exchange reaction, ethanol is a bad solvent for $CsPbBr_3$, meaning it does not dissolve the already formed PNCs on the film and TBAI being an ammonium salt dissolves readily in ethanol. The four butyl chains with TBAI makes it impossible to establish any hydrogen bond and upon reaction with the PNC film, the highly concentrated solution of TBAI forces out the Br form the solid film and replaces it with Iodine. We can thus see the brown color formation on our PNC film and upon UV illumination gives a bright luminescence. The difference between Route 1 and Route 2 is visible on the film as well as its property, as the route 1 film shows a PL of 649 nm and a greater stability of more than 3 hours while the route 2 synthesized anion exchanged film shows non-uniformity over the film and PL degrades over time within an hour but interestingly there is more red shift of 19 nm as compared to route1. The capping agent performs better in maintaining the stability when the anion source is introduced along with it to the perovskite film. The band energy of the anion exchanged films are centered at 1.93 and 1.88 eV.

3.4 Photoluminescence spectroscopic study

Table 4 shows the doped slides under daylight and under UV illumination

TABLE 4
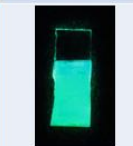
	CsPbBr$_3$	CsPbBr$_x$I$_{3-x}$	CsPbI$_x$Br$_{3-x}$	Anion exchange R1	Anion exchange R2
Visible light					
UV Illumination					

Fig 12: Photographs of synthesized PNCs under day light and under UV illumination λ_{ex}= 365nm.

The synthesized PNCs films shows bright luminescence under UV illumination at λ_{ex} = 365 nm. Films emitting at the visible range can be identified easily with our naked eyes as it is luminescent. The lead halide precursors are dissolved in DMF while the cesium halide salts were dissolved in Ethanol: water mixture solution. Equimolar mixing is required to get a red shift in the emission spectra. This is due to the addition of larger size Iodine into the system.
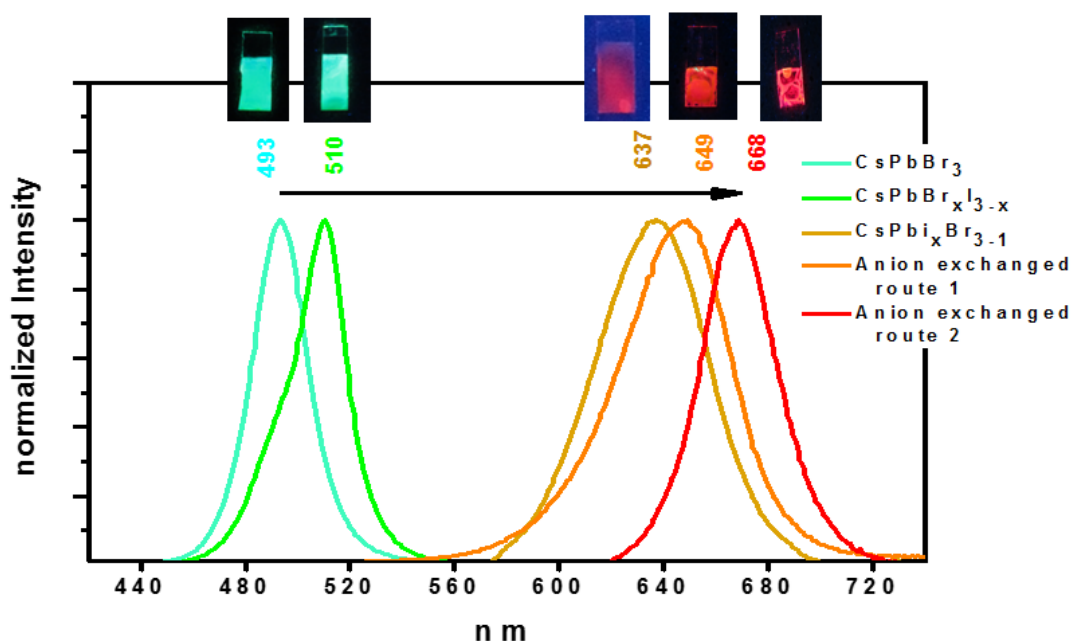
Fig13: Photoluminescence emission spectra of all the perovskite nanocrystals synthesized and the anion exchanged through different routes

The color gamut for emission has been tuned from green to red in the electromagnetic spectrum as shown in fig 13. The wide color gamut can be tuned easily with the change in composition and as for the solid state anion exchange the emission spectra can be tuned from 493 nm to 668 nm and the PLQY calculated table is represented in Table 5.

TABLE 5

Perovskites	PL-QY %
$CsPbBr_3$	55.90
$CsPbBr_xI_{3-x}$	19.88
$CsPbI_xBr_{3-x}$	20.92
Anion exchange Route 1	41.09
Anion exchange Route 2	49.77

PL-QY$= (ARs/ARr) (A_r/A_s) (n_s^2/n_r^2) * QY_R$

$ARS =$ integrated PL area under curve for sample

$AR_R=$ integrated PL area under curve for reference

$A_R=$ Absorbance at excitation wavelength of reference

$A_S=$ Absorbance at excitation wavelength of sample.

$n_s^2=$ Refracive index of the medium (sample)

$n_r^2=$ Refracive index of the medium (reference)

$QY_R =$ Quantum yield of the reference

3.4 Time correlated single photon count (TCSPC) lifetime measurement

Lifetime of the synthesized nano crystal films are short and this can be related to the size of the nano crystals formed, as surface charge trappers may be dominant. The PL decay fig 14 fits to tri exponential function with details given in Table 6. The exact mechanism contributing to the radiative recombination processes of the PNCs is difficult to discuss here.

TABLE 6

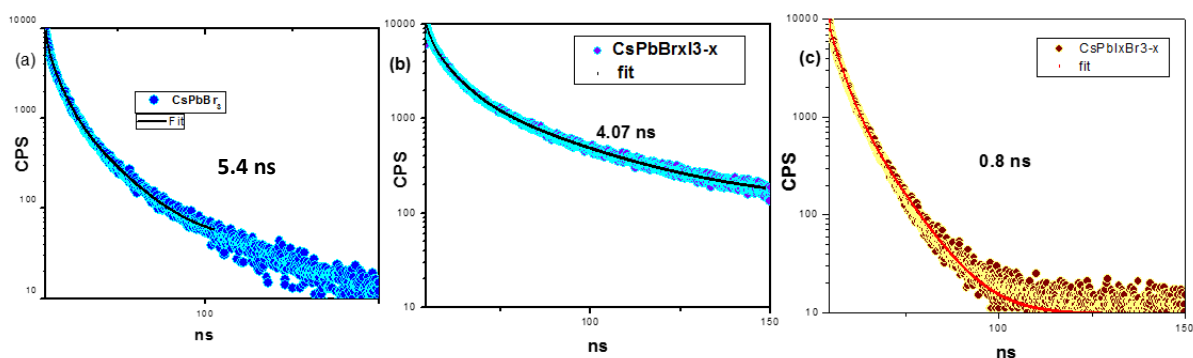| Perovskite	χ^2
$CsPbBr_3$	1.15
$CsPbBr_xI_{3-x}$	1.12
$CsPbI_xBr_{3-x}$	1.22

Fig 14: Lifetime measurement for the perovskites (a) $CsPbBr_3$ (b) $CsPbBr_xI_{3-x}$ (c) $CsPbI_xBr_{3-x}$

Conclusion

Our investigation on mesoporous alumina network on a film form to synthesize nanocrystals of CSPbBr$_3$ and its mixed halide components inside the pores has been successfully done. Maximum PL-QY was achieved at 55.9 %. The developed perovskite thin films maintain the uniformity over the film which in return can be used in applications of solar cells and LED based devices. Most importantly, solid state anion exchange could be performed in the films yielding tunability of the band gap over the entire visible range. Moreover, these PNC incorporated films show better stability in air which confirms that confinement of the NCs inside a mesoporous network helps to gain improved stability.

Future work

Work on fabrication of solar cells using the perovskite films is an ongoing process. Our hands will also extend in the application field of LED based devices from the developed uniform perovskite films as for potential backlit displays,

REFERENCES

1) Amgar, D., Aharon, S., & Etgar, L. **(2016).** Inorganic and Hybrid Organo-Metal Perovskite Nanostructures: Synthesis, Properties, and Applications. *Advanced Functional Materials*, *26*(47), 8576-8593.

2) Informationdisplay.org/IDArchive/2017/MarchApril/FrontlineTechnology Emerging Solution.aspx

3) Brandt, R. E.; Stevanovic, V.; Ginley, D. S.; Buonassisi, T. ́ Identifying Defect-Tolerant Semiconductors with High MinorityCarrier Lifetimes: beyond Hybrid Lead Halide Perovskites. MRS Commun. **2015**, 5, 265−275.

4) Song, J.; Li, J.; Li, X.; Xu, L.; Dong, Y.; Zeng, H. Quantum Dot Light-Emitting Diodes Based on Inorganic Perovskite Cesium Lead Halides (CsPbX3). Adv. Mater. **2015,** 27, 7162−7167.

5) Zhang, X.; Lin, H.; Huang, H.; Reckmeier, C.; Zhang, Y.; Choy, W. C. H.; Rogach, A. L. Enhancing the Brightness of Cesium Lead Halide Perovskite Nanocrystal Based Green Light-Emitting Devices through the Interface Engineering with Perfluorinated Ionomer. Nano Lett. **2016,** 16, 1415−1420.

6) Swarnkar, A.; Marshall, A. R.; Sanehira, E. M.; Chernomordik, B. D.; Moore, D. T.; Christians, J. A.; Chakrabarti, T.; Luther, J. M. Quantum Dot−Induced Phase Stabilization of α-CsPbI3 Perovskite for High-Efficiency Photovoltaics. Science **2016**, 354, 92−95.

7) Gonzalez-Carrero, S.; Galian, R. E.; Perez-Prieto, J. Organic- ́ Inorganic and All-Inorganic Lead Halide Nanoparticles. Opt. Express **2016**, 24, A285−A301

8) Bai, S.; Yuan, Z.; Gao, F. Colloidal Metal Halide Perovskite Nanocrystals: Synthesis, Characterization, and Applications. J. Mater. Chem. C **2016**, 4, 3898−3904.

9) Stoumpos, C. C.; Kanatzidis, M. G. Halide Perovskites: Poor Man's High-Performance Semiconductors. Adv. Mater. **2016**, 28, 5778−5793.

10) Manser, J. S.; Christians, J. A.; Kamat, P. V. Intriguing Optoelectronic Properties of Metal Halide Perovskites. Chem. Rev. **2016**, 116, 12956−13008.

11) Yang, G.-L.; Zhong, H.-Z. Organometal Halide Perovskite Quantum Dots: Synthesis, Optical Properties, and Display Applications. Chin. Chem. Lett. **2016**, 27, 1124−1130.

12) Zhang, Y.; Liu, J.; Wang, Z.; Xue, Y.; Ou, Q.; Polavarapu, L.; Zheng, J.; Qi, X.; Bao, Q. Synthesis, Properties, and Optical Applications of Low-Dimensional Perovskites. Chem. Commun. **2016**, 52, 13637−13655.

13)Amgar, D.; Aharon, S.; Etgar, L. Inorganic and Hybrid OrganoMetal Perovskite Nanostructures: Synthesis, Properties, and Applications. Adv. Funct. Mater. **2016,** 26, 8576−8593.

14) Huang, H.; Polavarapu, L.; Sichert, J. A.; Susha, A. S.; Urban, A. S.; Rogach, A. L. Colloidal Lead Halide Perovskite Nanocrystals: Synthesis, Optical Properties and Applications. NPG Asia Mater. **2016**, 8, e328.

15) Ha, S.-T.; Su, R.; Xing, J.; Zhang, Q.; Xiong, Q. Metal Halide Perovskite Nanomaterials: Synthesis and Applications. Chem. Sci. **2017**, 8, 2522−2536.

16) Li, X.; Cao, F.; Yu, D.; Chen, J.; Sun, Z.; Shen, Y.; Zhu, Y.; Wang, L.; Wei, Y.; Wu, Y.; et al. All Inorganic Halide Perovskites Nanosystem: Synthesis, Structural Features, Optical Properties and Optoelectronic Applications. Small **2017**, 13, 1603996.

17) Filippetti, A.; Mattoni, A. Hybrid Perovskites for Photovoltaics: Insights from First Principles. Phys. Rev. B: Condens. Matter Mater. Phys. **2014**, 89, 125203.

18) Brivio, F.; Frost, J. M.; Skelton, J. M.; Jackson, A. J.; Weber, O. J.; Weller, M. T.; Goñi, A. R.; Leguy, A. M. A.; Barnes, P. R. F.; Walsh, A. Phys. Rev. B: Condens. Matter Mater. Phys. **2015**, 92 (14), 144308.

19) Wang, H. C., Lin, S. Y., Tang, A. C., Singh, B. P., Tong, H. C., Chen, C. Y., ... & Liu, R. S. **(2016).** Mesoporous Silica Particles Integrated with All-Inorganic CsPbBr3 Perovskite Quantum-Dot Nanocomposites (MP-PQDs) with High Stability and Wide Color Gamut Used for Backlight Display. *Angewandte Chemie International Edition*, *55*(28), 7924-7929.

20) Dirin, D. N., Protesescu, L., Trummer, D., Kochetygov, I. V., Yakunin, S., Krumeich, F& Kovalenko, M. V**. (2016**). Harnessing defect-tolerance at the nanoscale: Highly luminescent lead halide perovskite nanocrystals in mesoporous silica matrixes. *Nano letters*, *16*(9), 5866-5874.

21) Wulff, G. (**1901**). Xxv. zur frage der geschwindigkeit des wachsthums und der auflösung der krystallflächen. *Zeitschrift für Kristallographie-Crystalline Materials*, *34*(1-6), 449-530.

22) Xu, C., Liu, J., & Tang, X**. (2009).** 2D shape matching by contour flexibility. *IEEE Transactions on Pattern Analysis and Machine Intelligence*, *31*(1), 180-186.

23) Mitzi, D. B. Solution-Processed Inorganic Semiconductors. J. Mater. Chem**. 2004**, 14, 2355−2365.

24) Mitzi, D. B.; Chondroudis, K.; Kagan, C. R. Organic-inorganic electronics. IBM J. Res. Dev. **2001**, 45, 29−45.

25) Mitzi, D. B.; Feild, C. A.; Harrison, W. T. A.; Guloy, A. M. Conducting Tin Halides with a Layered Organic-Based Perovskite Structure. Nature **1994,** 369, 467−469.

26) Mitzi, D. B.; Wang, S.; Feild, C. A.; Chess, C. A.; Guloy, A. M. Conducting Layered Organic-Inorganic Halides Containing (110)- Oriented Perovskites Sheets. Science **1995**, 267, 1473−1476.

27) W. S. Yang, B.-W. Park, E. H. Jung, N. J. Jeon, Y. C. Kim, D. U. Lee, S. S. Shin, J. Seo, E. K. Kim, J. H. Noh, S. I. Seok, Science **2017**, 356, 1376.

28) Li, D., Liao, P., Shai, X., Huang, W., Liu, S., Li, H., ... & Wang, M. **(2016).** Recent progress on stability issues of organic–inorganic hybrid lead perovskite-based solar cells. *RSC Advances*, *6*(92), 89356-89366.

29) Patent number   CN1101079A, 1995-04-05

30) Dandapat, A., Jana, D., & De, G**. (2011).** Pd nanoparticles supported mesoporous γ-Al2O3 film as a reusable catalyst for reduction of toxic CrVI to CrIII in aqueous solution. *Applied Catalysis A: General*, *396*(1-2), 34-39.

31) Pal, S., & De, G. (**2005**). A New Approach for the Synthesis of Au− Ag Alloy Nanoparticle Incorporated SiO2 Films. *Chemistry of materials*, *17*(24), 6161-6166.

32) Wulff, G. **(1901).** Xxv. zur frage der geschwindigkeit des wachsthums und der auflösung der krystallflächen. *Zeitschrift für Kristallographie-Crystalline Materials*, *34*(1-6), 449-530.